Supplementary Materials

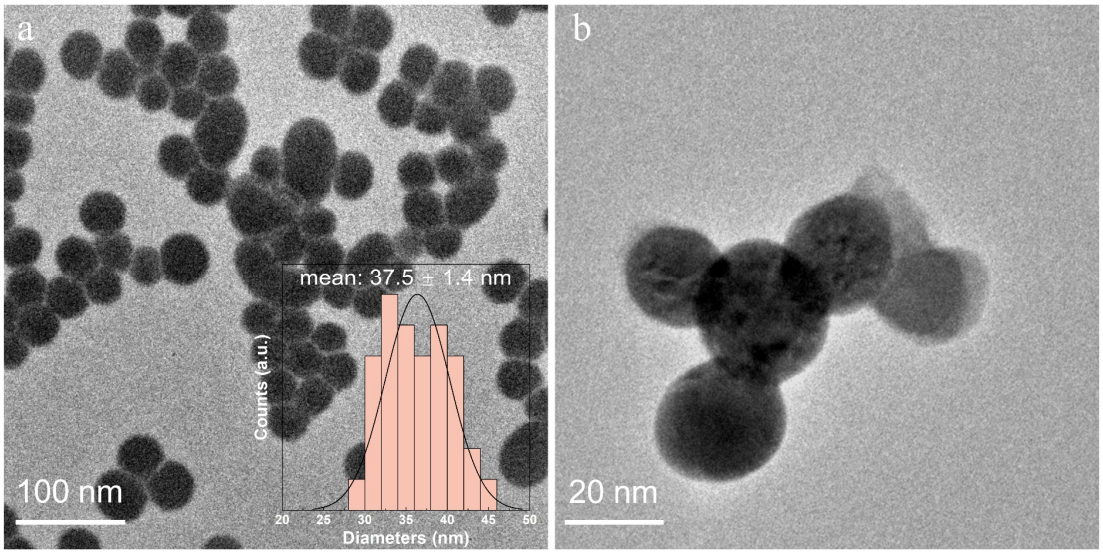

Figure S1. TEM images of Se nanoparticles in low magnification (**a**) and high magnification (**b**), synthesized following reported studies [1,2]. The size of Se nanoparticles is 37.5 ± 1.4 nm.

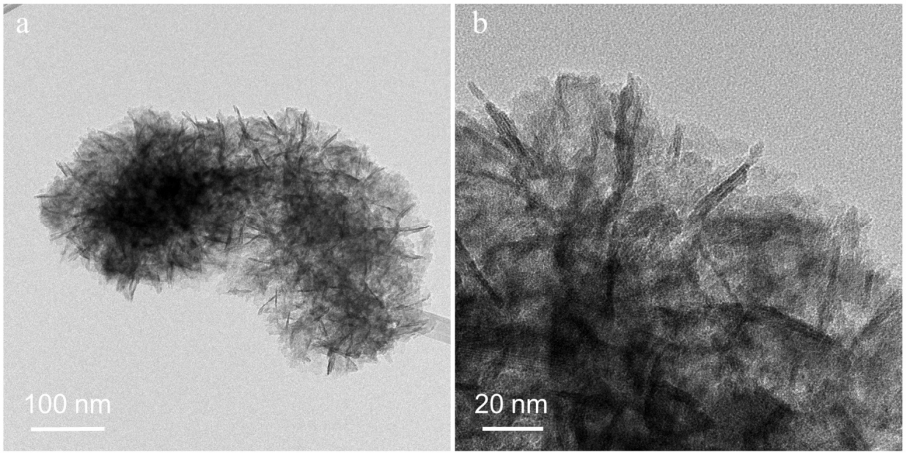

Figure S2. TEM images of $NiCoMoSeO_x$ nanosheets at low magnification (**a**) and high magnification (**b**).

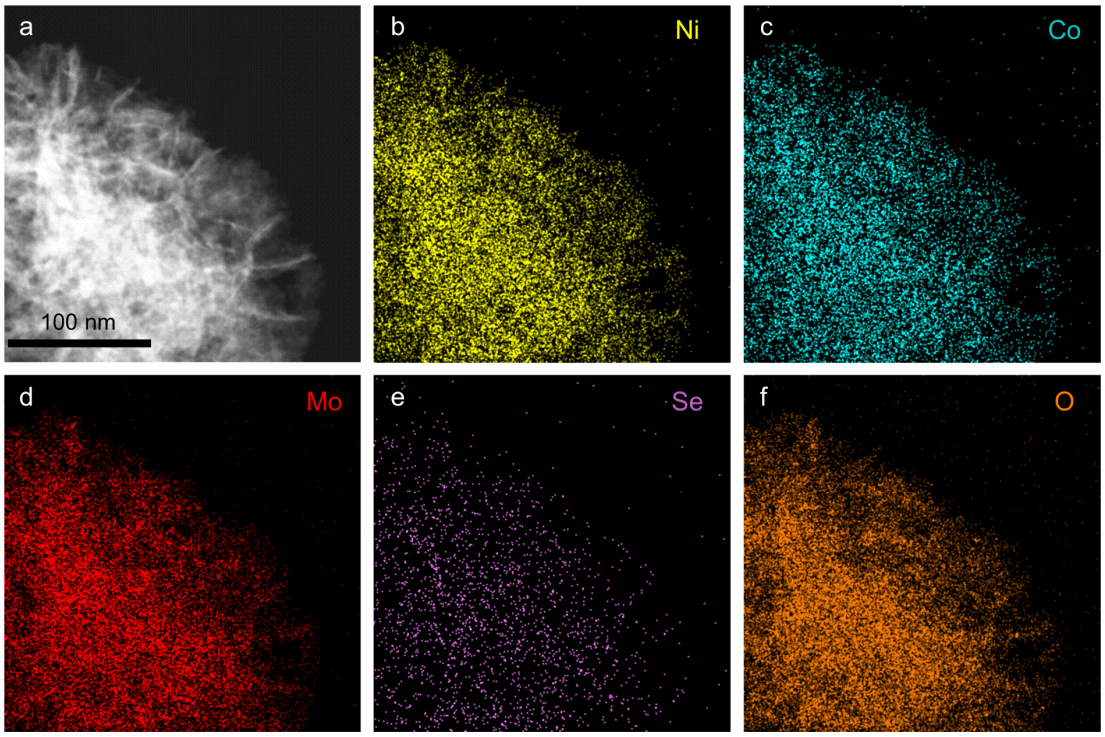

Figure S3. STEM image (**a**) and EDS elemental mapping of (**b**) Ni, (**c**) Co, (**d**) Mo, (**e**) Se, and (**f**) O distributions in the $NiCoMoSeO_x$ nanosheets. The scale bar applies to all panels in **a**.

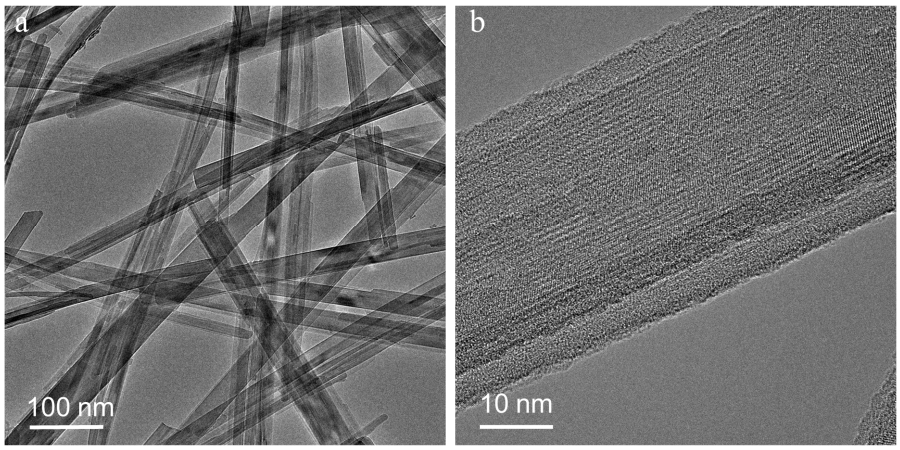

Figure S4. STEM images of $NiCoMoSeO_x$ nanorods at low magnification (**a**) and high magnification (**b**).

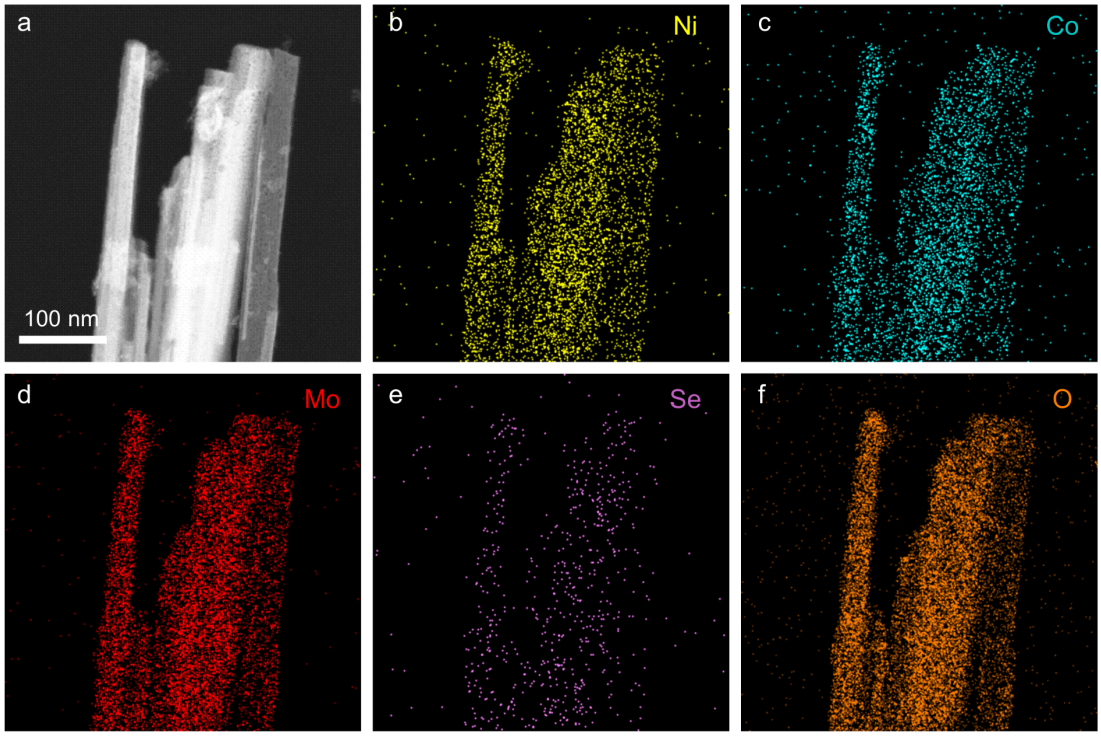

Figure S5. HADDF-STEM image (**a**) and EDS elemental mapping of (**b**) Ni, (**c**) Co, (**d**) Mo, (**e**) Se, and (**f**) O distributions in the $NiCoMoSeO_x$ nanorods. The scale bar applies to all panels in **a**.

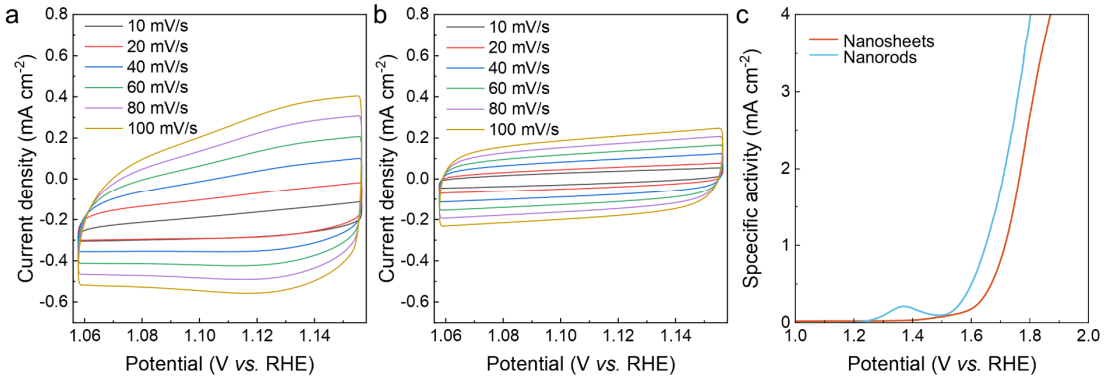

Figure S6. CVs of **(a)** nanorods and **(b)** nanosheets in the non-active potential range with scan rates of 10, 20, 40, 60, 80, 100 mV s^{-1}. **(c)** Specific activity of nanosheets and nanorods normalized by C_{dl}.

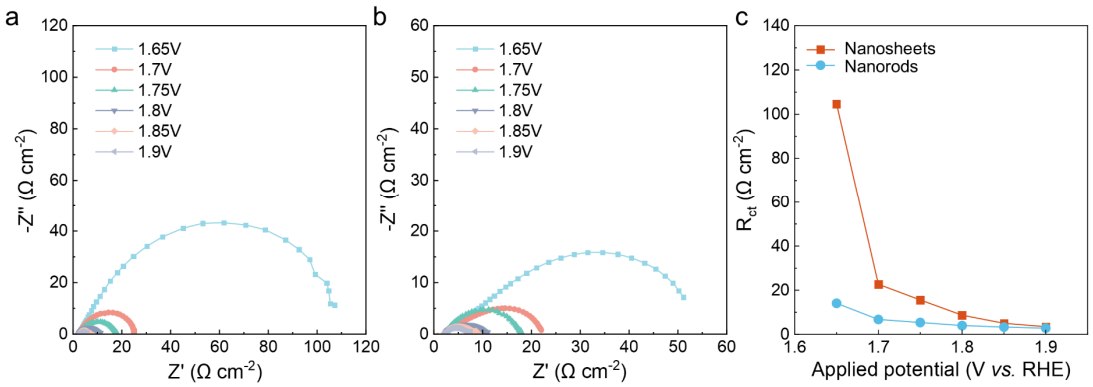

Figure S7. The Nyquist plots of nanosheets (**a**) and nanorods (**b**) measured at the range of 1.65–1.9 V. **(c)** The changes of R_{ct} upon different potentials derived from panel **a** and **b**.

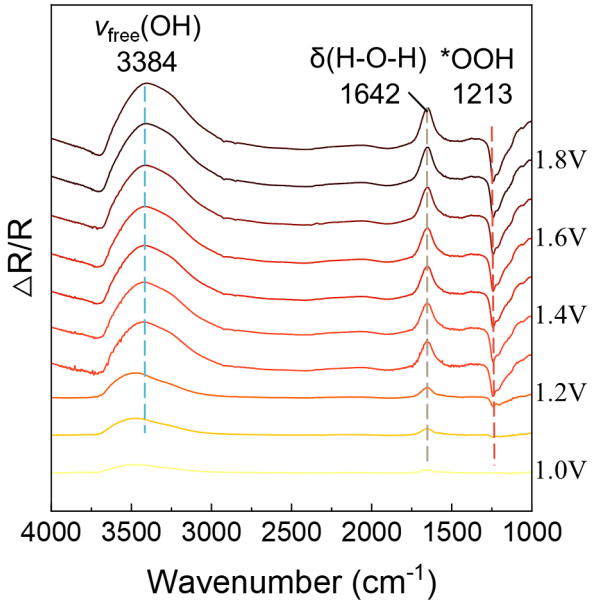

Figure S8 *In situ* ATR-SEIRAS spectra of RuO_2 during the OER at various potentials (1.0–1.9 V). The spectra highlight key vibrational bands: the free OH stretching at 3384 cm^{-1}, H-O-H bending at 1643 cm^{-1}, and adsorbed *OOH at 1213 cm^{-1}.[3]

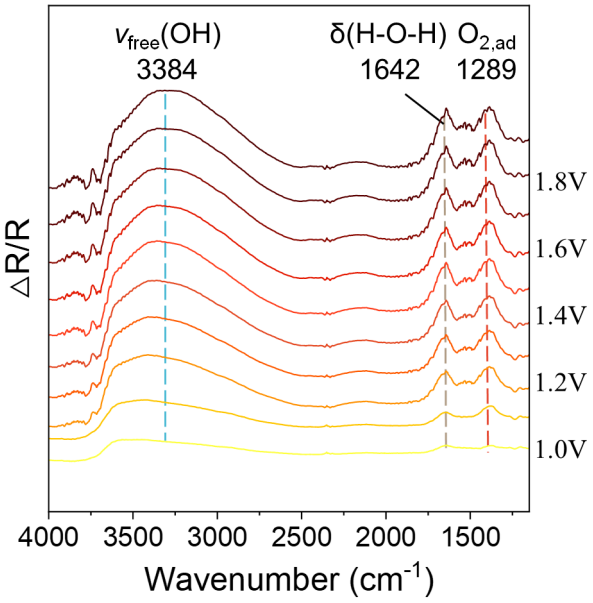

Figure S9 *In situ* ATR-SEIRAS spectra of Pt/C during the OER at various potentials (1.0–1.9 V). The spectra highlight key vibrational bands: the free OH stretching at 3384 cm^{-1}, H-O-H bending at 1642 cm^{-1}, and adsorbed O_2 at 1289 cm^{-1}.[4,5]

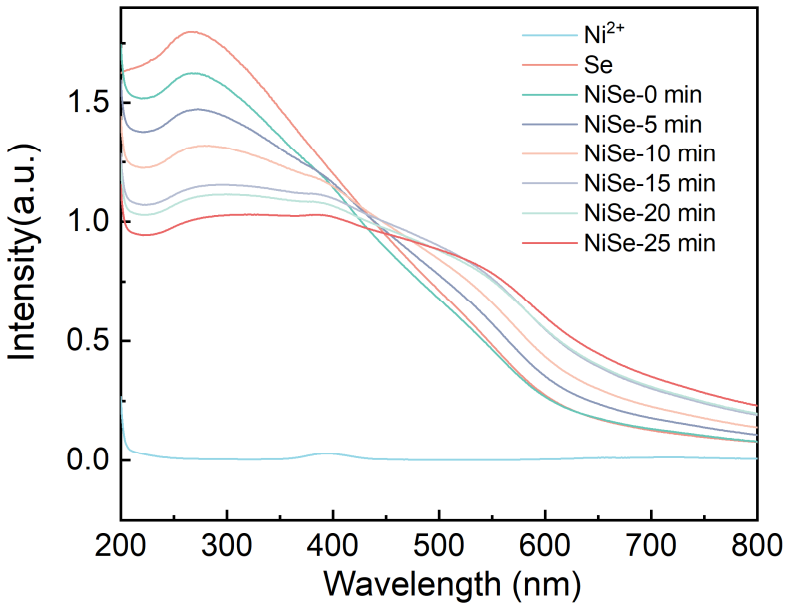

Figure S10. UV-Vis absorption spectra of Ni^{2+}, Se, and NiSe samples synthesized at different reaction times (0-25 min).

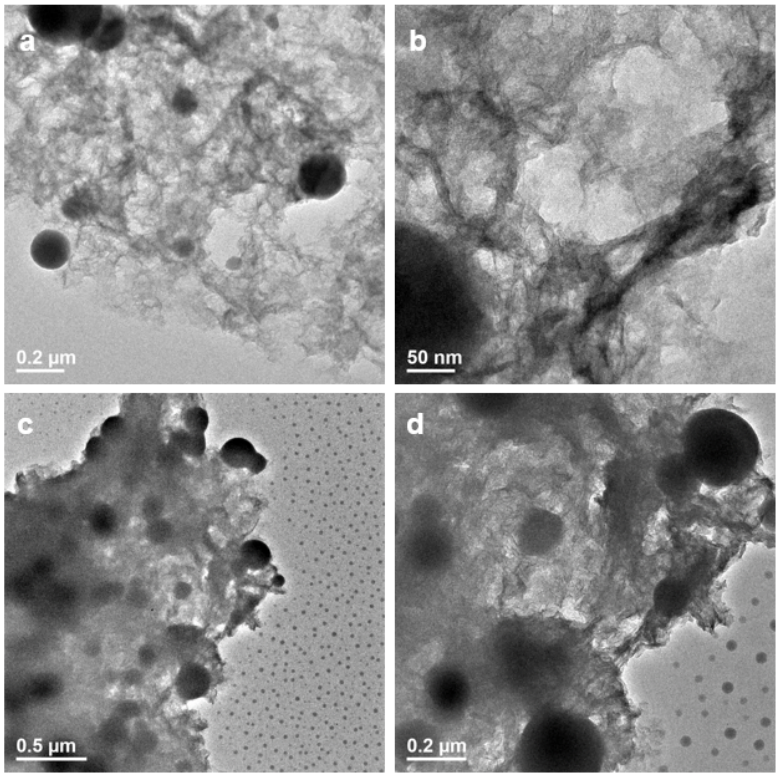

Figure S11. TEM images of NiCoSe trimetallic samples with different Ni/Co ratios: (a, b) Ni : Co : Se= 6:3:2 and (c, d) Ni : Co : Se= 20:3:2.

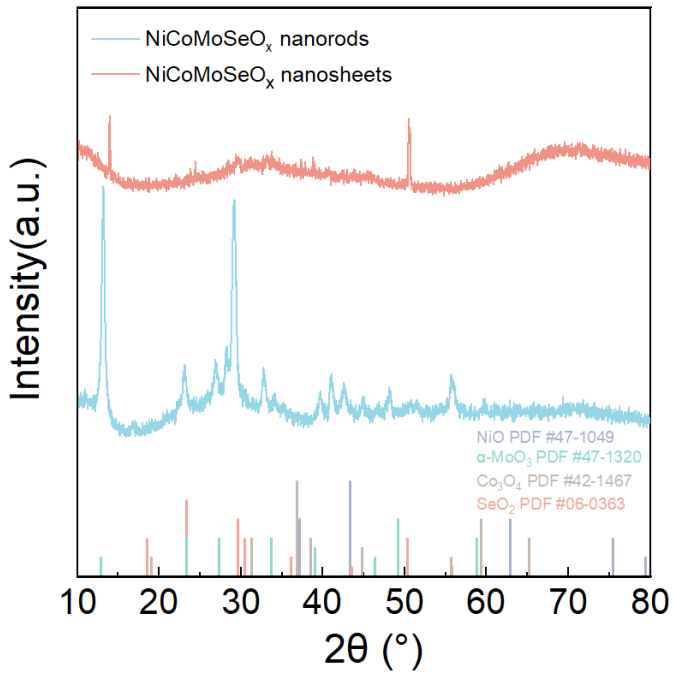

Figure S12. XRD patterns of NiCoMoSeOx nanorods (blue) and nanosheets (red), compared with standard reference cards of possible phases.

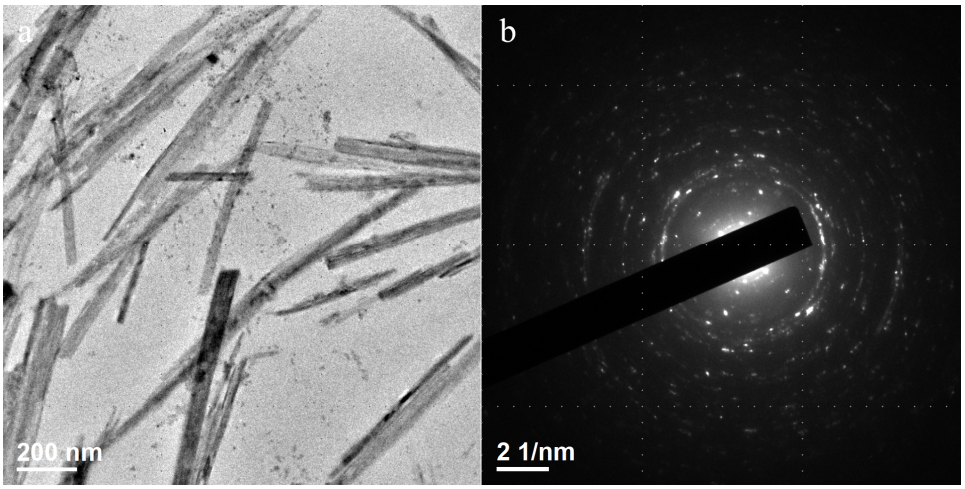

Figure S13. TEM image (**a**) and corresponding SAED pattern (**b**) of $NiCoMoSeO_x$ nanorods after 200 h of electrochemical durability testing.

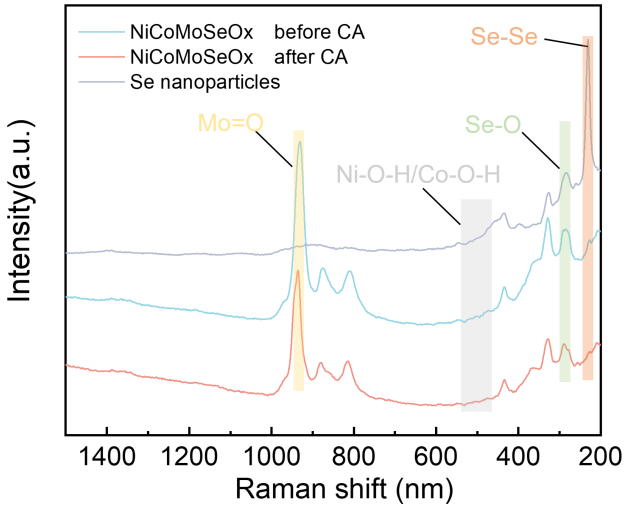

Figure S14. Raman spectra of $NiCoMoSeO_x$ before and after chronopotentiometry activation (CA), compared with Se nanoparticles.

References

1. Cheng, H.; Wang, C.; Lyu, Z.; Zhu, Z.; Xia, Y. Controlling the Nucleation and Growth of Au on A-Se Nanospheres to Enhance Their Cellular Uptake and Cytotoxicity. *J. Am. Chem. Soc.* **2023**, *145*, 1216–1226, https://doi:10.1021/jacs.2c11053.
2. Cheng, H.; Zhou, S.; Xie, M.; Gilroy, K.D.; Zhu, Z.; Xia, Y. Colloidal Nanospheres of Amorphous Selenium: Facile Synthesis, Size Control, and Optical Properties. *Chem. Nano. Mater.* **2021**, *7*, 620–625, https://doi:10.1002/cnma.202100115.
3. Chen, J.; Qi, M.; Yang, Y.; Xiao, X.; Li, Y.; Jin, H.; Wang, Y. Chloride Residues in RuO2 Catalysts Enhance Its Stability and Efficiency for Acidic Oxygen Evolution Reaction. *Angew. Chem. Int. Ed.* **2025**, *64*, e202420860, https://doi:10.1002/anie.202420860.
4. Miyake, H.; Ye, S.; Osawa, M. Electroless Deposition of Gold Thin Films on Silicon for Surface-Enhanced Infrared Spectroelectrochemistry. *Electrochem. Commun.* **2002**, *4*, 973–977, https://doi:10.1016/S1388-2481(02)00510-6.
5. Liu, X.; Zhao, P.; Liu, F.; Lin, R.; Yao, H.; Zhu, S. Attenuated Total Reflection Infrared Spectroscopy for Studying Electrochemical Cycling of Hydrogen, Carbon, and Nitrogen-Containing Molecules. *J. Energy Chem.* **2024**, *99*, 495–511, https://doi:10.1016/j.jechem.2024.08.008.